Journal of Systems Engineering and Electronics
Vol. 34, No. 5, October 2023, pp.1319 – 1332

TOA positioning algorithm of LBL system for underwater target based on PSO

XING Yao[1], WANG Jiongqi[1], HE Zhangming[1], ZHOU Xuanying[1], CHEN Yuyun[1,2], and PAN Xiaogang[3,*]

1. College of Liberal Arts and Sciences, National University of Defense Technology, Changsha 410073, China;
2. School of Mathematics and Big Data, Foshan University, Foshan 528000, China;
3. College of Systems Engineering, National University of Defense Technology, Changsha 410073, China

Abstract: For the underwater long baseline (LBL) positioning systems, the traditional distance intersection algorithm simplifies the sound speed to a constant, and calculates the underwater target position parameters with a nonlinear iteration. However, due to the complex underwater environment, the sound speed changes with time and space, and then the acoustic propagation path is actually a curve, which inevitably causes some errors to the traditional distance intersection positioning algorithm. To reduce the position error caused by the uncertain underwater sound speed, a new time of arrival (TOA) intersection underwater positioning algorithm of LBL system is proposed. Firstly, combined with the vertical layered model of the underwater sound speed, an implicit positioning model of TOA intersection is constructed through the constant gradient acoustic ray tracing. And then an optimization function based on the overall TOA residual square sum is advanced to solve the position parameters for the underwater target. Moreover, the particle swarm optimization (PSO) algorithm is replaced with the traditional nonlinear least square method to optimize the implicit positioning model of TOA intersection. Compared with the traditional distance intersection positioning model, the TOA intersection positioning model is more suitable for the engineering practice and the optimization algorithm is more effective. Simulation results show that the proposed methods in this paper can effectively improve the positioning accuracy for the underwater target.

Keywords: long baseline (LBL) positioning system, sound speed profile, constant gradient acoustic ray tracing, time of arrival (TOA) intersection model, particle swarm optimization (PSO).

DOI: 10.23919/JSEE.2023.000107

1. Introduction

With the requirement of underwater vehicle navigation, ocean exploration, ocean engineering, etc., it is necessary to locate the underwater target accurately [1−3]. The global navigation satellite system (GNSS) is the positioning system mainly based on the electromagnetic waves propagation. However, the electromagnetic waves attenuate quickly in the underwater environment, which cannot satisfy the requirement for the underwater positioning. Acoustic wave is the main form to be capable of long-distance underwater propagation, and the underwater propagation attenuation is much smaller than that of electromagnetic waves. Therefore, at present, the underwater acoustic positioning is the most widely used for the underwater target positioning [4].

According to the baseline length, underwater acoustic positioning systems mainly include the long baseline (LBL) positioning system, the short baseline (SBL) positioning system and the ultra-SBL (USBL) positioning system [5]. Due to the advantage of the long baseline, the higher positioning accuracy with the LBL system can be obtained for a relatively wide range [6]. Therefore, the LBL system is often used for higher-accuracy positioning for the underwater target. The time of arrival (TOA) of the acoustic signal propagation between the underwater target and the LBL system can be measured. The traditional positioning algorithm takes the underwater sound speed as a constant and multiplies the TOA and the sound speed to calculate the straight distance between the buoy and the underwater target [7−9], and then the underwater target position parameters can be calculated by using the optimal estimation methods [10−12].

Obviously, the main factors affecting the positioning accuracy of the LBL system include the buoy position error, the TOA measurement error and the sound speed error. The buoy position error and the TOA measurement

Manuscript received March 07, 2022.
*Corresponding author.
This work was supported by the National Natural Science Foundation of China (61903086; 61903366; 62001115), the Natural Science Foundation of Hunan Province (2019JJ50745; 2020JJ4280; 2021JJ40133), and the Fundamentals and Basic of Applications Research Foundation of Guangdong Province (2019A1515110136).

error can be compensated and corrected by means of the pre-calibration [13]. Due to the complex underwater environment such as seawater temperature, static pressure and seawater salinity, the underwater acoustic speed changes with time and space. Therefore, the sound speed error is the key factor to affect the positioning accuracy of the LBL system for the underwater target [14,15].

For the certain time, the sound speed mainly changes with water depth. The sound speed at different water depths can be measured directly by the sound velocity profiler (SVP) or calculated by the empirical formula with conductivity, temperature and density, etc. [16]. The change of underwater sound speed causes the actual propagation path of the underwater acoustic wave to be a curve. If the sound speed is simplified to a constant and the acoustic propagation path is simplified to a straight line, the sound speed error will directly affect the underwater target positioning accuracy of the LBL system.

Therefore, the sound speed correction is an effective means to improve the underwater positioning accuracy. At present, the researches on the sound speed correction mainly includes the following methods: weighted sound speed method, effective sound velocity table (ESVT) method [17], equivalent sound speed profile (ESSP) method [18,19], and ray tracing method [20,21], etc.

The weighted sound speed method calculates the sound speed by weighting the sound speed at different water depths according to the sound speed profile (SSP), and then obtains the straight distance according to the TOA, and finally solves the underwater target position parameters. This method is simple and also make the acoustic propagation path into a straight line. In addition, reference [22] assumed that the underwater sound speed is an unknown constant and uses unscented Kalman filter (UKF) algorithm to both estimate the underwater target position and the sound speed. However, this method is still based on the constant sound speed and the improvement for the positioning accuracy is limited.

The effective sound velocity (ESV) is the ratio of the straight distance between the two underwater points to the TOA. With the introduction of ESV, the curved propagation path is also equivalent to a straight line. The ESVT method is to establish the ESV as an ESVT related to the water depth distance and the horizontal distance between two underwater points according to the SSP. By measuring the depth and the TOA between the underwater target and the buoy, the underwater target position can be obtained by the interpolation and iteration algorithm. This method needs to build an ESVT in advance, and the underwater target depth also needs to be known. In addition, reference [23] presented a method for fitting the ESV without the SSP. This paper also assumed that the buoys are in the same horizontal plane and the underwater target depth is also known and then the ESV is fitted to a cubic polynomial related to the horizontal distance between the underwater target and the buoy. This method also required the underwater target depth to be known.

The ESSP method replaces the complex measured SSP with a simplified SSP. This method simplifies the measured SSP into an equivalent SSP with a constant gradient. In this way, the acoustic propagation path is simplified as an arc. The ESSP method is essentially an approximate model to the underwater sound speed. This model is simple and the applicability is poor when the incident angle of acoustic line is much larger.

The ray tracing method uses the SSP to track the acoustic signal propagation. The interval between two measured depths is called the layer. According to the different processing methods of the intra-layer sound speed, the acoustic ray tracing includes the constant speed acoustic ray tracing and the constant gradient acoustic ray tracing. The constant speed acoustic ray tracing assumes that the sound speed in each layer is constant, and the constant gradient acoustic ray tracing assumes that the sound speed in the layer varies linearly with the water depth. The acoustic ray tracing method can be used to achieve higher-accuracy underwater positioning. However, the ray tracing method requires the incident angle of acoustic line to be known, so it cannot be directly applied to the underwater positioning.

The traditional distance intersection positioning model regards the underwater sound speed as a constant, and there is an inevitable sound speed error to calculate the straight distance, which directly affect the positioning accuracy for the underwater target. In addition, the acoustic ray tracing method requires a known incident angle, which cannot be directly applied to the underwater positioning. Aiming at the above problems, with the SSP in the test area and the constant gradient acoustic ray tracing, this paper proposes a new TOA intersection positioning algorithm of underwater LBL system based on particle swarm optimization (PSO).

The main contributions of this paper are as follows:

(i) The TOA measured by the LBL system is established as an implicit function related to the two underwater points (the underwater target and the buoy) and the SSP with the constant gradient acoustic ray tracing. Therefore, the traditional distance intersection positioning model is converted to a TOA intersection positioning

model. Different from the traditional distance intersection positioning model, this model directly uses the TOA to solve the position parameter for the underwater target without the straight distance, which avoids the sound speed error, thereby improving the positioning accuracy. In addition, the proposed TOA intersection positioning model can locate the underwater target without the known incident angle of acoustic ray.

(ii) An optimization function of the implicit positioning model is constructed based on the TOA residuals square sum to calculate the optimal estimation for the underwater target position parameters. According to the implicit function of TOA positioning intersection model, the TOA calculation data between the buoy and the underwater target at each moment is obtained. The TOA residuals square sum is calculated by making the difference between the TOA calculation data and the TOA measurement data.

(iii) Due to the optimization function is an implicit expression, the traditional least square method is not suitable. Therefore, an intelligent optimization algorithm is adopted to solve the implicit function. The decreasing inertia weight based on Gaussian function is adopted to avoid the PSO algorithm falling into the local optimal solution. The function can be minimized to obtain the optimal position estimation for the underwater target.

The rest structure of this paper is as follows: Section 2 introduces the principle of LBL positioning system, and presents two traditional distance intersection positioning algorithms. Section 3 presents the TOA intersection positioning model based on constant gradient acoustic ray tracing, and theoretically analyzes the feasibility of the implicit positioning model. Section 4 constructs an optimization function based on the overall TOA residuals square sum, and get the optimal position estimate for the underwater target through the PSO algorithm. The simulation is conducted in Section 5. Finally, the conclusions are drawn in Section 6.

2. LBL positioning system based on distance intersection

2.1 LBL system measurement principle

The coordinate system is established, as shown in Fig. 1. A point within the detection range of the LBL system is set as the origin $\boldsymbol{O}=[0,0,0]^{\mathrm{T}}$ with the ox axis towards east and the oy axis towards north, the oz axis completes the triad. Assume that there are n (n>3) buoys arranged on the sea surface. Suppose $\boldsymbol{X}_i=[x_i,y_i,z_i]^{\mathrm{T}}(i=1,2,\cdots,n)$ are the corresponding positions in this coordinate system, and $\boldsymbol{X}=[x,y,z]^{\mathrm{T}}$ is the position of the underwater target.

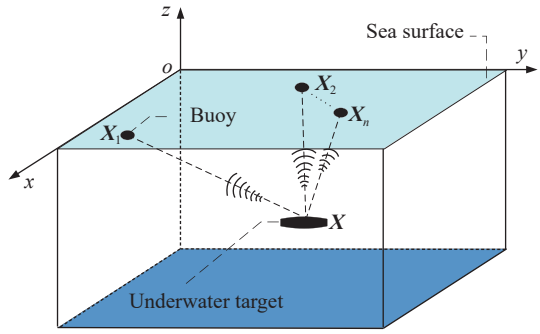

Fig. 1 LBL system

Each buoy is equipped with an acoustic receiver to obtain the acoustic signal, and the underwater target is equipped with an acoustic emitter. Assume that the receiver and the emitter are time-synchronized, and the time of the acoustic signal emitted by the underwater target is known. According to the time that the buoy receives the acoustic signal, the TOA t_i of the acoustic signal propagating from the underwater target $\boldsymbol{X}$ to the ith buoy $\boldsymbol{X}_i$ can be measured.

2.2 Positioning model based on weighted sound speed

According to the TOA t_i of the LBL system, the straight distance R_i from the underwater target $\boldsymbol{X}$ to the buoy $\boldsymbol{X}_i$ can be written as

$$R_i=ct_i \tag{1}$$

where c is the underwater sound speed.

According to the SSP, the sound speed c in (1) can be calculated by the weighted sound speed method, and (2) is the expression of the weighted sound speed.

$$\bar{c}=\frac{1}{H}\sum_{j=1}^{m-1}\frac{(c_j+c_{j+1})(h_{j+1}-h_j)}{2} \tag{2}$$

where H is the sea depth as shown in Fig. 2, and c_j is the sound speed at the water depth h_j.

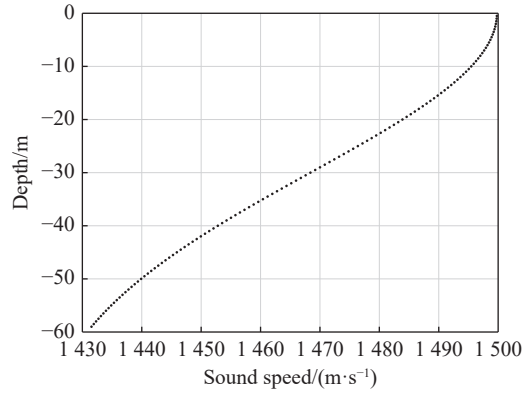

Fig. 2 Diagram of SSP

Combined with (1) and (2), the straight distance R_i between the underwater target and the ith buoy can be calculated through the geometric relationship between the underwater target $\boldsymbol{X}$ and the buoy $\boldsymbol{X}_i$, which is expressed as

$$R_i = \sqrt{(x-x_i)^2+(y-y_i)^2+(z-z_i)^2}. \tag{3}$$

According to (1) and (3), the positioning model based on the weighted sound speed can be written as

$$\begin{cases} \bar{c}t_1 = \sqrt{(x-x_1)^2+(y-y_1)^2+(z-z_1)^2} \\ \bar{c}t_2 = \sqrt{(x-x_2)^2+(y-y_2)^2+(z-z_2)^2} \\ \quad\vdots \\ \bar{c}t_n = \sqrt{(x-x_n)^2+(y-y_n)^2+(z-z_n)^2} \end{cases}. \tag{4}$$

The geometry relationship consisting of the points that the distance to the buoy $\boldsymbol{X}_i$ is R_i, which is a sphere whose center is $\boldsymbol{X}_i$ and the radius is R_i. When the number of buoys is more than three, the unique underwater target position can be calculated as shown in Fig. 3.

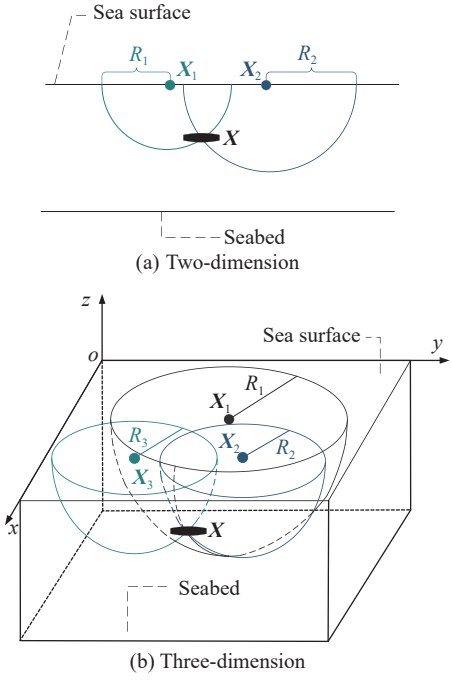

Fig. 3 Distance intersection model

The sound speed is considered as a constant sound speed in the weighted sound speed method. However, due to the complex environment under the sea, the underwater sound speed changes with time and space. Although this method uses the SSP, the weighted sound speed is still an approximation of the underwater sound speed, which inevitably contains the sound speed error.

Therefore, the positioning model based on the identification of the sound speed error needs to be constructed. The positioning accuracy of the distance intersection model can be improved through identifying the sound speed error contained in (4).

2.3 Positioning model based on sound speed error identification

Due to the variety of the underwater sound speed, the sound speed error is inevitable in the positioning model when the weighted sound speed is taken as the underwater sound speed. Assume that the sound speed error in the positioning model (4) is Δc and the corresponding distance error is $\Delta R_i (i = 1,2,\cdots,n)$. Note that the number of buoys in this model should be more than four to ensure that the model can be solved. According to (1), the distance error can be obtained.

$$\Delta R_i = \Delta c t_i \tag{5}$$

where t_i is the TOA measurement data related to the buoy $\boldsymbol{X}_i$.

Assume that the distance measurement data is R_i and the real distance is $\widehat{R}_i$, the geometric relationship between the underwater target $\boldsymbol{X}$ and the buoy $\boldsymbol{X}_i$ can be expressed as

$$R_i = \widehat{R}_i + \Delta R_i. \tag{6}$$

According to (1) and (6), the positioning model with the sound speed error identification is as follows:

$$\begin{cases} \bar{c}t_1 = \sqrt{(x-x_1)^2+(y-y_1)^2+(z-z_1)^2} + \Delta c t_1 \\ \bar{c}t_2 = \sqrt{(x-x_2)^2+(y-y_2)^2+(z-z_2)^2} + \Delta c t_2 \\ \quad\vdots \\ \bar{c}t_n = \sqrt{(x-x_n)^2+(y-y_n)^2+(z-z_n)^2} + \Delta c t_n \end{cases}. \tag{7}$$

The identification error is added in this model, which can improve the positioning accuracy. Besides, the computational complexity is basically the same compared with the weighted sound speed method. However, the positioning model based on the identification of the sound speed error still essentially assumes the sound speed to be a constant. Therefore, the improvement of the positioning accuracy in this distance intersection model is also limited.

2.4 Solution by Gauss-Newton method

It is evident that the model (7) is nonlinear and the underwater target position parameters can be solved through the Gauss-Newton method.

Let that

$$\boldsymbol{R} = [R_1, R_2, \cdots, R_n]^{\mathrm{T}}, \tag{8}$$

$$\boldsymbol{f}=[\widehat{R}_1+\Delta R_1,\widehat{R}_2+\Delta R_2,\cdots,\widehat{R}_n+\Delta R_n]^{\mathrm{T}}, \tag{9}$$

$$\boldsymbol{e}=\boldsymbol{R}-\boldsymbol{f}. \tag{10}$$

Then the Jacobian matrix of $\boldsymbol{f}$ can be denoted as $\boldsymbol{J}$, which is written as follows:

$$\boldsymbol{J}=\begin{bmatrix} \dfrac{(x-x_1)}{R_1} & \dfrac{(y-y_1)}{R_1} & \dfrac{(z-z_1)}{R_1} & t_1 \\ \dfrac{(x-x_2)}{R_2} & \dfrac{(y-y_2)}{R_2} & \dfrac{(z-z_2)}{R_2} & t_2 \\ \vdots & \vdots & \vdots & \vdots \\ \dfrac{(x-x_n)}{R_n} & \dfrac{(y-y_n)}{R_n} & \dfrac{(z-z_n)}{R_n} & t_n \end{bmatrix} \tag{11}$$

where R_i denotes the straight distance between the buoy $\boldsymbol{X}_i$ and the underwater target $\boldsymbol{X}$.

Assume that $\boldsymbol{\beta}=[x,y,z,\Delta c]^{\mathrm{T}}$, and the expression of the function F is as follows:

$$F(\boldsymbol{\beta}+\Delta\boldsymbol{\beta})=\frac{1}{2}\boldsymbol{e}^{\mathrm{T}}(\boldsymbol{\beta}+\Delta\boldsymbol{\beta})\boldsymbol{e}(\boldsymbol{\beta}+\Delta\boldsymbol{\beta}). \tag{12}$$

In order to obtain the gradient vector $\Delta\boldsymbol{\beta}$ to make $F(\boldsymbol{\beta}+\Delta\boldsymbol{\beta})$ descent faster, the partial derivative of $F(\boldsymbol{\beta}+\Delta\boldsymbol{\beta})$ with respect to $\Delta\boldsymbol{\beta}$ is calculated through

$$\frac{\partial}{\partial\Delta\boldsymbol{\beta}}F(\boldsymbol{\beta}+\Delta\boldsymbol{\beta})=-\boldsymbol{J}^{\mathrm{T}}\boldsymbol{e}+\boldsymbol{J}^{\mathrm{T}}\boldsymbol{J}\Delta\boldsymbol{\beta}. \tag{13}$$

And then the gradient descent direction $\Delta\boldsymbol{\beta}$ can be obtained:

$$\Delta\boldsymbol{\beta}=\lambda\left(\boldsymbol{J}^{\mathrm{T}}\boldsymbol{J}\right)^{-1}\boldsymbol{J}^{\mathrm{T}}\boldsymbol{e},\ \ \lambda>0. \tag{14}$$

The accuracy $\varepsilon_{\min}$ and the maximum iteration number $k_{\max}$ can be set in advance. By substituting the approximate initial value $(x_0,y_0,z_0,\Delta c_0)$ into (14), the optimal estimation for $\boldsymbol{\beta}$ can be obtained.

If the initial value is inappropriate, the iteration will not converge or converge to the wrong solution. Therefore, selecting an appropriate initial value is the premise to ensure the iteration converge to the correct solution. The least square method is relatively simple and has low computational complexity whose accuracy is sufficient for solving the initial value. Therefore, the least square method is adopted to obtain the initial value.

The initial value (x_0,y_0,z_0) of the underwater target position parameters can be calculated through the least square method.

Equation (3) can be transformed as

$$R_1^2=(x-x_1)^2+(y-y_1)^2+(z-z_1)^2, \tag{15}$$

$$\begin{cases} R_2^2=(x-x_2)^2+(y-y_2)^2+(z-z_2)^2 \\ \quad\vdots \\ R_n^2=(x-x_n)^2+(y-y_n)^2+(z-z_n)^2 \end{cases}. \tag{16}$$

If the buoys are not on the same horizontal plane, the quadratic term of the unknown parameter can be eliminated by making the difference between (15) and (16). Thus, the following simplified equation can be obtained:

$$\begin{bmatrix} x_1-x_i \\ y_1-y_i \\ z_1-z_i \end{bmatrix}^{\mathrm{T}}\begin{bmatrix} x \\ y \\ z \end{bmatrix}=\frac{1}{2}\left(R_i^2-R_1^2+\|\boldsymbol{X}_1\|^2-\|\boldsymbol{X}_i\|^2\right). \tag{17}$$

Denote that

$$\boldsymbol{A}=\begin{bmatrix} x_1-x_2 & y_1-y_2 & z_1-z_2 \\ x_1-x_3 & y_1-y_3 & z_1-z_3 \\ \vdots & \vdots & \vdots \\ x_1-x_n & y_1-y_n & z_1-z_n \end{bmatrix}, \tag{18}$$

$$\boldsymbol{Y}=\frac{1}{2}\begin{bmatrix} R_2^2-R_1^2+\|\boldsymbol{X}_1\|^2-\|\boldsymbol{X}_2\|^2 \\ R_3^2-R_1^2+\|\boldsymbol{X}_1\|^2-\|\boldsymbol{X}_3\|^2 \\ \vdots \\ R_n^2-R_1^2+\|\boldsymbol{X}_1\|^2-\|\boldsymbol{X}_n\|^2 \end{bmatrix}. \tag{19}$$

And then (17) can be rewritten as

$$\boldsymbol{A}\boldsymbol{X}=\boldsymbol{Y}. \tag{20}$$

Then the least square estimation for (20) is

$$\boldsymbol{X}=\left(\boldsymbol{A}^{\mathrm{T}}\boldsymbol{A}\right)^{-1}\boldsymbol{A}^{\mathrm{T}}\boldsymbol{Y}. \tag{21}$$

Note that if the detection range of the LBL system is small, the curvature of the sea surface can be ignored. Under this condition, all the buoys are on the sea surface, that is, $z_i\approx z_j(i\neq j)$, and then the coefficient matrix $\boldsymbol{A}$ is rank-deficient. In this case, (17) is shown as

$$\begin{bmatrix} x_1-x_2 & y_1-y_2 \\ x_1-x_3 & y_1-y_3 \\ \vdots & \vdots \\ x_1-x_n & y_1-y_n \end{bmatrix}\begin{bmatrix} x \\ y \end{bmatrix}= \frac{1}{2}\begin{bmatrix} R_2^2-R_1^2+x_1^2+y_1^2-x_2^2-y_2^2 \\ R_3^2-R_1^2+x_1^2+y_1^2-x_3^2-y_3^2 \\ \vdots \\ R_n^2-R_1^2+x_1^2+y_1^2-x_n^2-y_n^2 \end{bmatrix}. \tag{22}$$

Similarly, the least square estimation (x_0,y_0) for (22) can be obtained. Further, the water depth z_0 of the underwater target can be calculated by substituting (x_0,y_0) into (3), and the initial value (x_0,y_0,z_0) can also be obtained.

Remark 1 The premise of the distance intersection positioning algorithm of the underwater LBL system is to assume that the underwater sound speed is a constant and the acoustic propagation path is a straight line. However, due to the variety of sound speed caused by the complex underwater environment, the acoustic propagation path from the underwater target $\boldsymbol{X}$ to the buoy $\boldsymbol{X}_i$ is a curve as Fig. 4.

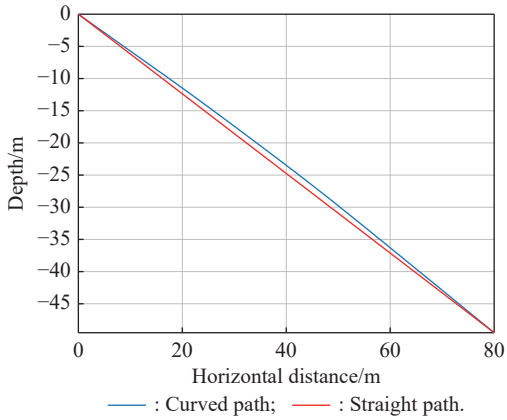

Fig. 4 Real curved path VS approximated straight line

If the sound speed is regarded as a constant, the sound speed error will be inevitable in the positioning model based on the distance intersection. Therefore, in this paper, an implicit TOA intersection underwater positioning model is constructed based on the SSP and the constant gradient acoustic ray tracing. Different from the distance intersection positioning model, this positioning model directly uses the SSP and the TOA to calculate the underwater target position without calculating the straight distance from the underwater target $\boldsymbol{X}$ to the buoy $\boldsymbol{X}_i$, thereby avoiding the position error caused by the sound speed error.

3. TOA intersection positioning model of LBL system

3.1 Acoustic ray tracing

The sound speed underwater has two characteristics: the vertical distribution and the horizontal distribution. In open water, the change of the sound speed in the vertical direction is 2−3 orders of the magnitude faster than that in the horizontal direction. In the small test area, the change of the sound speed in the horizontal direction usually is small. Therefore, it can be assumed that the sound speed remains constant at the same water depth.

For the certain time, assume that the sound speed only changes with the water depth, and the sound speed remains constant at the same water depth. In other words, the sound speed is a function of the water depth, and it is called the vertical layered model. The vertical layered model is an approximation to the change of the sound speed in the sea and it is the basic assumption to solve the problem of the long-range acoustic propagation. In the vertical layered model, the variety of the sound speed along the vertical depth is the SSP. The SSP is generally complex and changes with the underwater environment.

The sound speed change causes the refraction of the acoustic ray, so that the actual acoustic propagation path is a continuously changing curve. Effectively eliminating the influence of the acoustic ray refraction can improve the underwater positioning accuracy. When the SSP is known, the acoustic ray tracing is an effective way to eliminate the acoustic ray refraction.

At present, there are two methods of the acoustic ray tracing, namely, the constant speed acoustic ray tracing and the constant gradient acoustic ray tracing. The first method assumes that the sound speed in the layer remains unchanged, and the second method assumes that the sound speed in the layer changes linearly with the water depth. Although both of the above ray tracing methods are the approximations of the SSP, the constant gradient acoustic ray tracing is more in line with the change of the sound speed, whose accuracy is also higher. However, the incident angle of the acoustic ray is usually unknown in the underwater positioning test, so the ray tracing methods cannot be directly applied to the underwater positioning. Therefore, with the SSP and the constant gradient acoustic ray tracing, an implicit TOA intersection underwater positioning model is constructed to obtain the underwater target position.

3.2 Implicit TOA intersection positioning model

Assume that the sound speed in the sea satisfies the vertical layered model. Suppose $[h_j, h_{j+1}]$ is the interval of the water depth in the jth layer, and $[c_j, c_{j+1}]$ is the interval of the sound speed in $[h_j, h_{j+1}]$. The acoustic ray incident angle is assumed as $\theta_j (j = 1, 2, \cdots, m)$, as shown in Fig. 5.

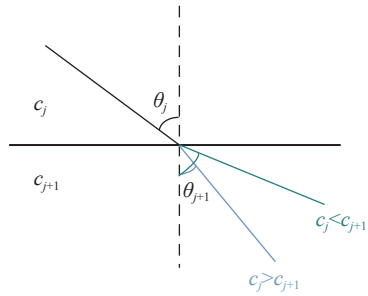

Fig. 5 Refraction of the acoustic ray

According to Snell's Law of the ray acoustics [4], the sound speed and the incidence angle satisfy:

$$\frac{\sin\theta_1}{c_1} = \frac{\sin\theta_2}{c_2} = \cdots = \frac{\sin\theta_m}{c_m} = p \tag{23}$$

where p is an unknown constant, and the incident angle θ_j is the angle between the vertical direction and the propagation direction of the acoustic ray at the water depth h_j.

According to Snell's Law, (23) can be deduced as follows:

$$\frac{\sin\theta}{c}=p\Rightarrow \mathrm{d}\sin\theta=p\cdot\mathrm{d}c\Rightarrow\cos\theta\cdot\mathrm{d}\theta=p\cdot\mathrm{d}c\Rightarrow$$
$$\frac{\mathrm{d}h}{\mathrm{d}s}\cdot\mathrm{d}\theta=p\cdot\mathrm{d}c\Rightarrow\frac{\mathrm{d}\theta}{\mathrm{d}s}=p\frac{\mathrm{d}c}{\mathrm{d}h} \tag{24}$$

where s is the length of the acoustic propagation path, and h is the water depth.

Thus, the curvature of the acoustic propagation path in the jth layer is as follows:

$$\frac{\mathrm{d}\theta}{\mathrm{d}s}=p\frac{\mathrm{d}c}{\mathrm{d}h}. \tag{25}$$

Assume that the sound speed in the layer changes with a constant gradient, and $\mathrm{d}c/\mathrm{d}h=(c_{j+1}-c_j)/r(h_{j+1}-h_j)=g_j$ is a constant in the jth layer. The radius r_j of the path is shown as

$$r_j=\frac{\mathrm{d}s}{\mathrm{d}\theta}=\frac{1}{pg_j}. \tag{26}$$

That is, the curvature of the acoustic propagation path is a constant and the acoustic propagation path is an arc in the jth layer.

As shown in Fig. 6, the horizontal distance l_j and the vertical distance h_j of the acoustic propagation path in the jth layer are (27) and (28), respectively.

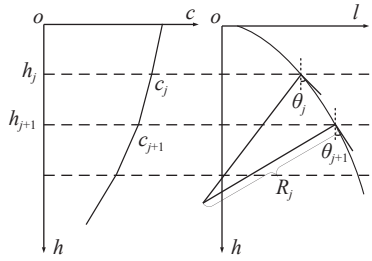

Fig. 6 Constant gradient acoustic ray tracing

$$\eta_j=\frac{1}{pg_j}(\cos\theta_j-\cos\theta_{j+1}), \tag{27}$$

$$\zeta_j=\frac{1}{pg_j}(\sin\theta_{j+1}-\sin\theta_j). \tag{28}$$

According to the geometric relationship between the ith buoy $\boldsymbol{X}_i=[x_i,y_i,z_i]^{\mathrm{T}}$ and the underwater target $\boldsymbol{X}=[x,y,z]^{\mathrm{T}}$, we can obtain the following equations:

$$\sqrt{(x-x_i)^2+(y-y_i)^2}=\sum\eta_j, \tag{29}$$

$$\sqrt{(z-z_i)^2}=\sum\zeta_j. \tag{30}$$

The propagation time of the acoustic signal in the jth layer can be written as

$$t_j=\int\frac{\mathrm{d}s}{c}. \tag{31}$$

Due to the propagation path of the acoustic ray in the jth layer is an arc, the length of the acoustic propagation path in the layer can be expressed as (32) by using (23) and (26).

$$s_j=r_j(\theta_{j+1}-\theta_j)=r_j[\arcsin(pc)-\theta_j] \tag{32}$$

In the jth layer, the interval of the sound speed c is $[(\sin\theta_j)/p,(\sin\theta_{j+1})/p]$, and (31) can be written as

$$t_j=\int_{(\sin\theta_j)/p}^{(\sin\theta_{j+1})/p}\frac{Rp}{c\sqrt{1-p^2c^2}}\mathrm{d}c. \tag{33}$$

Further, let $\xi=pc$, then the interval of ξ is $[\sin\theta_j,\sin\theta_{j+1}]$. Equation (33) can be rewritten as

$$t_j=\int_{\sin\theta_j}^{\sin\theta_{j+1}}\frac{Rp}{\xi\sqrt{1-\xi^2}}\mathrm{d}\xi=$$
$$\frac{1}{g_j}\ln\left(\frac{\sin\theta_{j+1}}{\sin\theta_j}\cdot\frac{1+\sqrt{1-\sin^2\theta_j}}{1+\sqrt{1-\sin^2\theta_{j+1}}}\right)=$$
$$\frac{1}{g_j}\left[\ln\left(\tan\frac{\theta_{j+1}}{2}\right)-\ln\left(\tan\frac{\theta_j}{2}\right)\right]. \tag{34}$$

If the SSP and the positions of two underwater points (the buoy $\boldsymbol{X}_i$ and the underwater target $\boldsymbol{X}$) are known, the incident angle of the acoustic ray can be calculated according to (29) and (30), and moreover, the TOA of the acoustic propagation can be calculated according to (34). Thus, the TOA is an implicit function related to the SSP and the positions of two underwater points (the buoy $\boldsymbol{X}_i$ and the underwater target $\boldsymbol{X}$), which is expressed as follows:

$$T_i=f(c(h_1,h_2,\cdots,h_m),\boldsymbol{X},\boldsymbol{X}_i) \tag{35}$$

where $c(h_1,h_2,\cdots,h_m)$ is the SSP in the test area, and f is the implicit function.

According to (35), combined with the measurement data of the LBL system, the implicit TOA intersection positioning model of the LBL system for the underwater target is constructed as follows:

$$\begin{cases}T_1=f(c(h_1,h_2,\cdots,h_m),\boldsymbol{X},\boldsymbol{X}_1)\\T_2=f(c(h_1,h_2,\cdots,h_m),\boldsymbol{X},\boldsymbol{X}_2)\\\quad\vdots\\T_n=f(c(h_1,h_2,\cdots,h_m),\boldsymbol{X},\boldsymbol{X}_n)\end{cases} \tag{36}$$

where T_i is the TOA measured by the ith buoy $\boldsymbol{X}_i(i=1,2,\cdots,n)$, and n is the number of buoys in the LBL system.

When the number of buoys is more than three, the unique underwater target position can be determined, as shown in Fig. 7. Unlike the distance intersection model, the geometry in the TOA intersection model is not spherical and the expression is implicit.

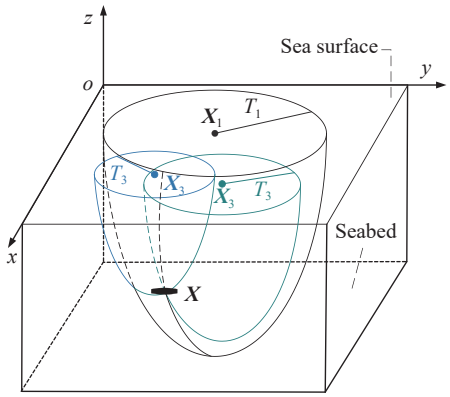

Fig. 7 TOA intersection model

Remark 2 Due to the complex underwater environment, the underwater sound speed changes with time and space, and the acoustic propagation path is a curve. The distance intersection model regards the underwater sound speed as a constant, and assumes the acoustic propagation path to be a straight line, resulting in poorer positioning accuracy. The TOA intersection positioning model proposed uses the vertical layered property of the sound speed in the sea, and calculates the TOA of the acoustic propagation between two underwater points with the SSP. Compared with the traditional distance intersection positioning model, the TOA intersection positioning model is more suitable for the engineering practice.

4. Position parameters solution with PSO

4.1 Optimization criteria construction

In Section 3, we construct a TOA intersection positioning model based on the constant gradient acoustic ray tracing. Different from the traditional distance intersection positioning model, the time parameter in the TOA intersection positioning model is an implicit function related to the SSP, the underwater target position and the buoy position. Thus, the underwater target position cannot be solved by the traditional least square method, but it can be solved by the intelligent optimization algorithms that not rely on an explicit function.

Similar to the traditional distance intersection positioning model, when the number of buoys in the TOA intersection positioning model is more than three, the unique underwater target position can be obtained. Therefore, the overall TOA residual square sum is constructed as the optimization index and the underwater target position parameters are the corresponding variables to be optimized. The optimization algorithm is used to iterate continuously to reduce the overall TOA residual square sum. When the overall TOA residual square sum is the smallest, the solution is the optimal estimation for the underwater target position parameters.

The TOA measurement data between the underwater target and the buoy $\boldsymbol{X}_i$ at the qth moment is denoted as T_{iq}, and the TOA calculation data is denoted as T'_{iq}. The TOA residuals square sum at the qth moment is

$$\mathrm{RSS}_q = \sum_{i=1}^{n} \left\| T_{iq} - T'_{iq} \right\|^2. \tag{37}$$

The TOA residual square sum of N moments is denoted as a vector **RSS**.

$$\mathbf{RSS} = [\mathrm{RSS}_1, \mathrm{RSS}_2, \cdots, \mathrm{RSS}_N] \tag{38}$$

Then the optimization function (the overall TOA residual square sum) is expressed as

$$g(\boldsymbol{X}) = \|\mathbf{RSS}\|_2 = \sqrt{\sum_{q}^{N} \mathrm{RSS}_q^2}. \tag{39}$$

Since T'_{iq} in (37) is an implicit function related to the SSP and the positions of two underwater points, the optimization function cannot be solved by the traditional least square method. The PSO algorithm is simple to implement with higher accuracy, which can be used to solve the position parameters of the underwater target. Therefore, this paper uses the PSO algorithm to solve the optimization function.

4.2 Principle of PSO

The PSO algorithm is proposed by Eberhart and Kennedy [24], which originated from the research on the predation of birds. It uses the information sharing of individuals in the group to make the particle swarm evolve from disorder to order in the search space, so as to obtain the optimal solution to the problem.

The PSO algorithm uses the iterative method to search for the optimal solution of the particles in the search space and finds the global optimal solution by iterating the current optimal value. The PSO algorithm is simple to implement with high accuracy in a high convergence speed. In recent years, the PSO algorithm has been widely studied and developed, and it has shown its superiority in solving different optimization problems [25,26].

The PSO algorithm is based on the $\mathrm{iter}_{\max}$ iterations of solving a large number N_{pso} of the random particles in the search space. Each particle has position $\boldsymbol{\Psi}_\rho (\rho = 1, 2, \cdots)$. N_{PSO} and velocity $\boldsymbol{v}_\rho$ and is a candidate solution to the optimization problem. The overall TOA residuals square sum is called the fitness value, and all of the parti-

cles have a fitness value. Denote $\mathbf{Pb}_\rho^k$ is the particle best position, which is the best solution of the ρth particle has achieved so far in k iterations. Denote $\mathbf{Gb}^k$ is the global best position, which is the best solution obtained by the whole swarm in k iterations. The particle updates its position and velocity by tracking the particle best position and the global best position in the iteration. The particle iterates in the search area. If the particle position parameter is outside the search area, the particle position parameter is replaced by the corresponding boundary value. The equations of the PSO algorithm in the kth iteration are as follows:

$$\begin{cases} \boldsymbol{v}_\rho^{k+1} = w\boldsymbol{v}_\rho^k + \mu_1\iota_1\left(\mathbf{Pb}_\rho^k - \boldsymbol{\Psi}_\rho^k\right) + \mu_2\iota_2\left(\mathbf{Gb}^k - \boldsymbol{\Psi}_\rho^k\right) \\ \boldsymbol{\Psi}_\rho^{k+1} = \boldsymbol{\Psi}_\rho^k + \boldsymbol{v}_\rho^{k+1} \end{cases} \tag{40}$$

where w denotes the inertia weight, which reflects the influence of the velocity of the previous iteration and weighs the local search and the global search capabilities of the particle, and μ_1, μ_2 are the learning factors that are non-negative constants, and ι_1, ι_2 are random number that uniformly distributed within $[0, 1]$.

When using the PSO algorithm to solve the TOA intersection model, the initial positions of the particle swarm are randomly selected in the search area. The particle position in (40) represents the underwater target position to be iterated in the search area. And the velocity is the position iteration step size in the optimization process.

The inertia weight controls the influence of the historical velocity on the current velocity. When the inertia weight obeys the normal distribution, the global search ability of the algorithm can be improven and the algorithm can be prevented from falling into the local optimal solution. Therefore, the PSO algorithm with decreasing the inertia weight based on Gaussian function is used to optimize the TOA intersection model [27], and the expression of the inertia weight in the kth iteration is shown as

$$w(t) = (w_{\max} - w_{\min})\mathrm{e}^{-\frac{k^2}{(\phi\times \mathrm{iter}_{\max})^2}} + w_{\min} \tag{41}$$

where ϕ is the expansion constant, which leads to the change rate of the inertia weight, and $w_{\max}, w_{\min}$ are the maximum inertia weight and the minimum inertia weight, respectively.

The flow chart of the TOA positioning algorithm of the LBL system for the underwater target based on the PSO algorithm is shown in Fig 8.

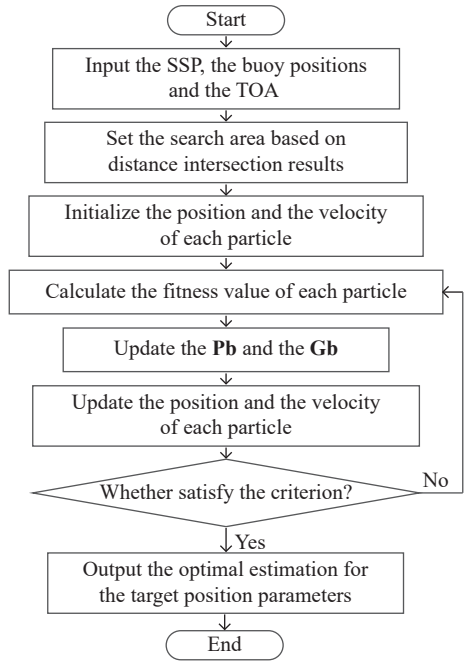

Fig. 8 Process of the TOA positioning algorithm of LBL system based on PSO

5. Simulation

In this section, we construct an offshore measurement scene of the LBL system. The random errors are added to the TOA and the buoy positions in the scene to implement two numerical simulations.

The first simulation is to solve the underwater target trajectory. In order to verify the effectiveness of the algorithm proposed in this paper, the result of TOA positioning algorithm (named M3) is compared with that of the two distance intersection positioning algorithms, i.e., the distance intersection positioning algorithm based on the weighted sound speed (named M1), the distance intersection positioning algorithm based on the identification of the sound speed error (named M2) in Section 2.

The second simulation is to analyze the positioning accuracy in the test area. By using the algorithm proposed in this paper, the solution errors calculated by (42) at different positions can be obtained, and the positioning accuracy in the test area can be analyzed.

$$\|\Delta \boldsymbol{X}\| = \sqrt{(\hat{x}-x)^2 + (\hat{y}-y)^2 + (\hat{z}-z)^2} \tag{42}$$

where $[\hat{x}, \hat{y}, \hat{z}]^{\mathrm{T}}$ is the optimal estimation for the underwater target position parameters $[x, y, z]^{\mathrm{T}}$.

5.1 Numerical simulation 1 (positioning accuracy comparison)

(i) Set the test scene: eight buoys of LBL system are arranged on the sea surface, and the positions are shown in Table 1.

Table 1 Buoy positions

Buoy	x/m	y/m	z/m
1	100	100	−1
2	100	−100	−1
3	−100	100	−1
4	−100	−100	−1
5	50	0	−1
6	0	50	−1
7	−50	0	−1
8	0	−50	−1

In this simulation, due to the short movement time of the underwater target, a cubic polynomial can be used to constrain the underwater target trajectory. The constraint equation is as follows:

$$\begin{cases} x = a_3t^3 + a_2t^2 + a_1t + a_0 \\ y = b_3t^3 + b_2t^2 + b_1t + b_0 \\ z = c_3t^3 + c_2t^2 + c_1t + c_0 \end{cases} . \tag{43}$$

The spatial relative relationship between the buoys and the underwater target trajectory is shown in Fig. 9.

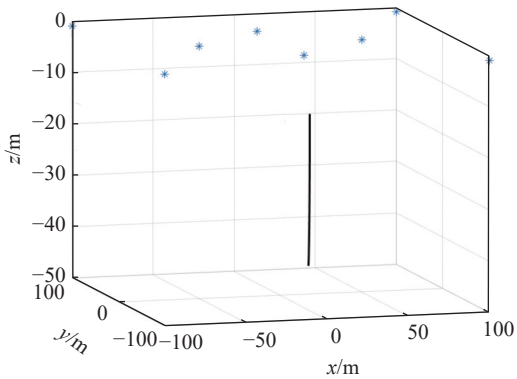

(a) Buoy positions and the target trajectory

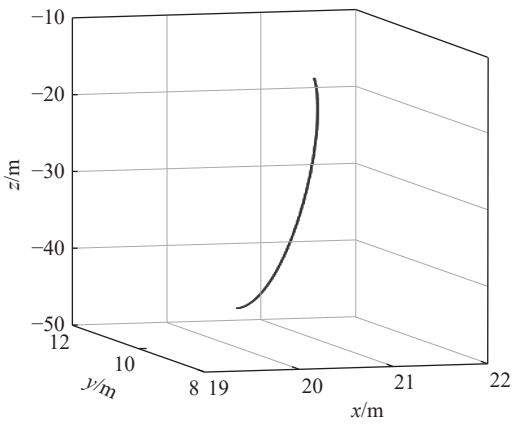

(b) Target trajectory

*: Buoy positions; ——: Target trajectory.

Fig. 9 LBL system and the target trajectory

Assume that the buoys and the underwater target are time-synchronized, and the errors caused by time asynchrony can be ignored. The frequency of the acoustic signal sent by the underwater target is 50 Hz, and the time of sending the signal is known. The buoy can measure the TOA of the acoustic signal from the underwater target to the buoy by receiving the signal.

(ii) Measurement data simulation: the SSP used in the simulation is shown in Fig. 10, and the TOA of the acoustic signal from the underwater target to the buoy can be calculated by (35). Suppose that random errors of the TOA and the buoy position obey the normal distribution with zero-mean and the standard deviation is 30 μs and 0.1 m, respectively.

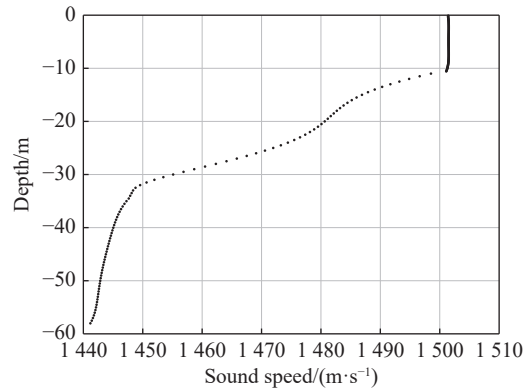

Fig. 10 Sound speed profile

(iii) The distance intersection positioning algorithm based on the weighted sound speed: using (2) with the SSP, we can calculate the weighted sound speed is 1 477.7 m/s. According to the TOA measurement data, the straight distance R_i between the underwater target $\boldsymbol{X}$ and the buoy $\boldsymbol{X}_i$ can be calculated by (1). The initial value of the underwater target position $\hat{\boldsymbol{X}}_0$ can be calculated according to (21), and the underwater target position parameters $\hat{\boldsymbol{X}}_1$ can be obtained by using the Gauss-Newton method.

(iv) The distance intersection positioning algorithm based on the identification of the sound speed error: the weighted sound speed and the TOA measurement data are used to calculate the straight distance measurement values R_i'. The initial value of the underwater target position $\hat{\boldsymbol{X}}_0$ can be calculated, and the initial value of the sound speed error is assumed to be 0. The underwater target position parameters $\hat{\boldsymbol{X}}_2$ and the sound speed error Δc can be obtained by using the Gauss-Newton method.

(v) The TOA intersection positioning algorithm: the underwater target position parameters $\hat{\boldsymbol{X}}_2$ that obtained by the distance intersection positioning algorithm based on the identification of the sound speed error are the initial values, and the search space is selected around the initial values. 50 initial particles are randomly selected in the search space. Using the SSP and (35), the fitness value of each particle can be calculated. Iterate the particle posi-

tion continuously to find the particle with the minimal of the overall TOA residuals square sum, that is, the optimal estimation $\hat{\boldsymbol{X}}_3$ for the underwater target position parameters $\boldsymbol{X}$.

According to the above simulation process, the trajectories obtained by different positioning algorithms are shown in Fig. 11.

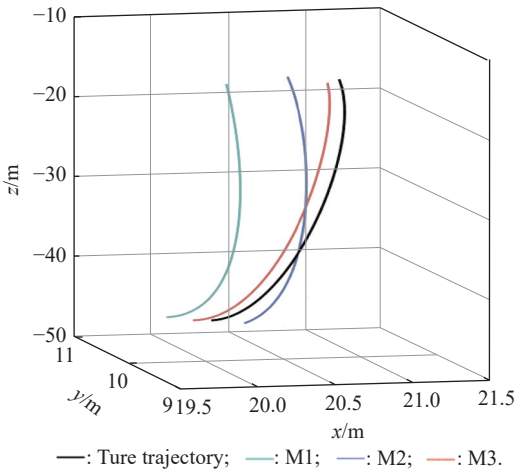

Fig. 11 Trajectories solved by each algorithm

Let the solution error in the x,y,z direction be $\Delta x,\Delta y,\Delta z$, respectively and the position error be $\Delta\boldsymbol{X}$. Fig. 12 shows the errors for different algorithms.

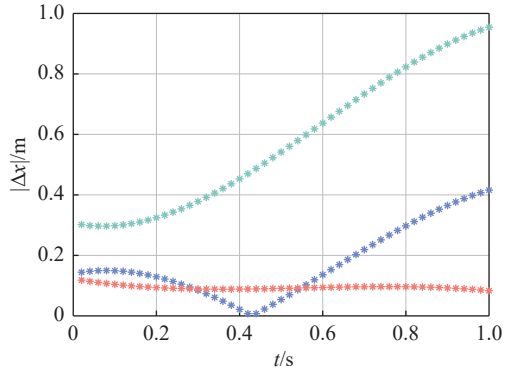

(a) Error in x direction

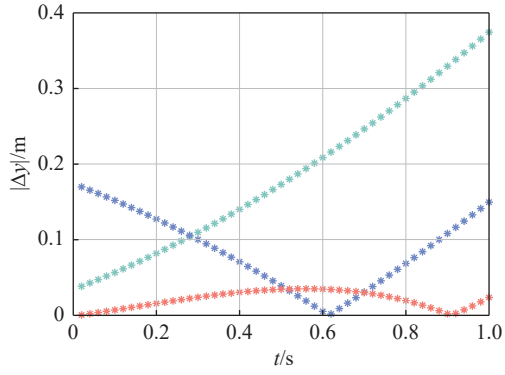

(b) Error in y direction

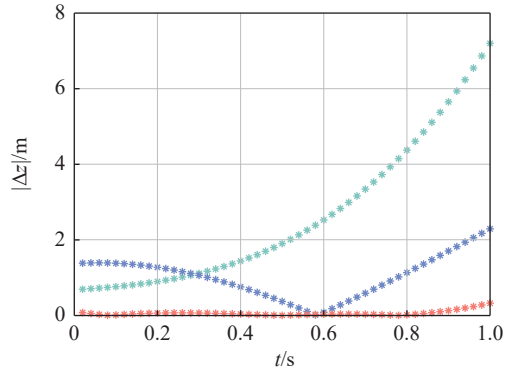

(c) Error in z direction

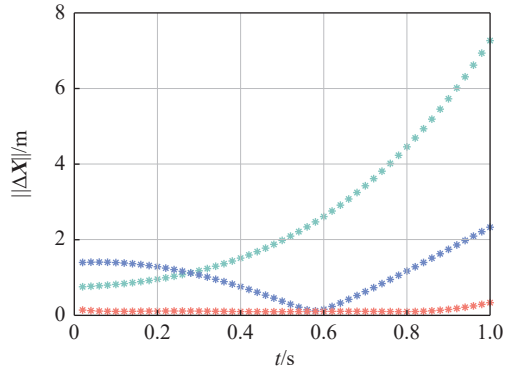

(d) Position Error

*: M1; *: M2; *: M3.

Fig. 12 Errors of each algorithm

The statistical error results of each positioning algorithm are presented in Table 2.

Table 2 Statistical error results of each algorithm

Algorithm	$\overline{\lvert\Delta x\rvert}$/m	$\overline{\lvert\Delta y\rvert}$/m	$\overline{\lvert\Delta z\rvert}$/m	$\overline{\lVert\Delta\boldsymbol{X}\rVert}$/m
M1	0.5778	0.1869	2.6452	2.7210
M2	0.1757	0.0858	1.0234	1.0506
M3	0.0944	0.0211	0.0593	0.1233

Fig. 13 shows the change of the overall TOA residual square sum in the iteration of the PSO algorithm.

From the simulation results, it can be seen that:

(i) In the presence of the random errors in the TOA and the buoy positions, M1 has the worst accuracy, and the average position error is about 2 m. After identifying the sound speed error, the average position error of M2 is reduced to about 1 m. M3 proposed in this paper has a much better performance and the average position error is about 0.1 m. Compared with M1 and M2, the positioning accuracy of M3 is greatly improven.

(ii) As shown in Fig. 13, at the beginning of the iteration, the overall TOA residual square sum decreased significantly, and after 15 iterations, the overall TOA residual square sum decreased slowly and tended to be stable.

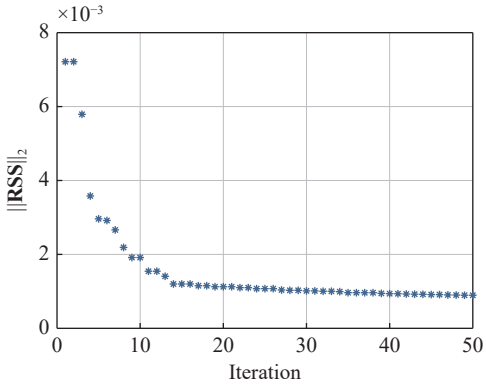

Fig. 13 Change of the $\|\mathbf{RSS}\|_2$ in the iteration

5.2 Numerical simulation 2 (accuracy space of the test area)

(i) Set the test scene: as in the numerical simulation 1, eight buoys are arranged on the sea surface. The water depth z of the test area is -50 m, and $x,y\in[-150\text{ m},150\text{ m}]$. The underwater targets are selected evenly within the test area. The LBL system can measure the TOA of the acoustic ray propagates from the underwater target to the buoy by receiving the acoustic signal.

(ii) Measurement data simulation: generate measurement data. In this simulation, the SSP used is shown in Fig. 10. According to the underwater target position and the buoy positions, the TOA can be calculated by using (35), and the random errors are the same as the errors in numerical simulation 1.

(iii) Calculate the positioning accuracy: the position error in the test area can be calculated by the M1, M2, and M3. Repeat the above process 50 times to get the average position error.

According to the above process, the positioning accuracy (accuracy space) of each positioning algorithm in the test area can be calculated and the results are shown in Fig. 14.

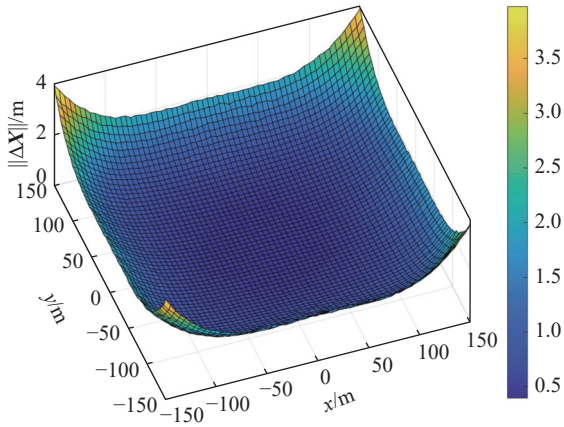

(a) Positioning accuracy of M1

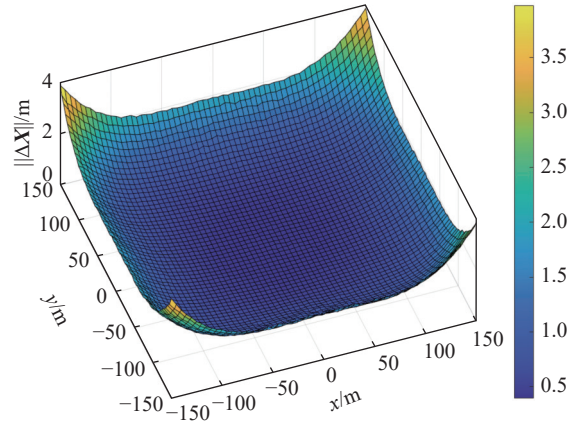

(b) Positioning accuracy of M2

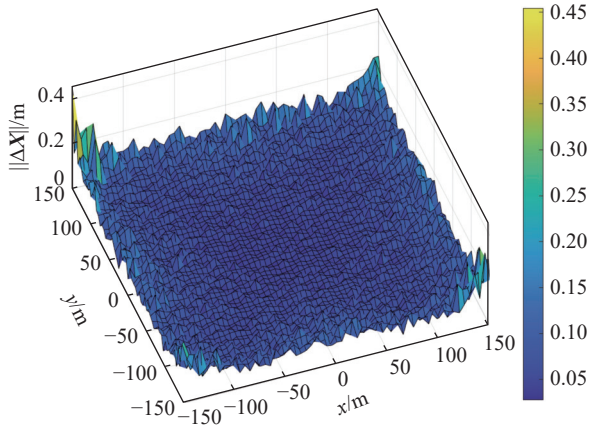

(c) Positioning accuracy of M3

Fig. 14 Positioning accuracy at the water depth of −50 m

The average position error results of each positioning algorithm are presented in Table 3.

Table 3 Average position error of each algorithm

Algorithm	$\overline{\lvert\Delta x\rvert}$/m	$\overline{\lvert\Delta y\rvert}$/m	$\overline{\lvert\Delta z\rvert}$/m	$\overline{\lVert\Delta\boldsymbol{X}\rVert}$/m
M1	0.5384	0.5377	0.5146	0.9186
M2	0.2166	0.2169	0.3720	0.4820
M3	0.0288	0.0288	0.0507	0.0650

From the simulation results, it can be seen that:

(i) In the test area, the average position error of M1 is about 0.92 m, which is the largest among the three algorithms. After identifying the sound speed error, the average position error of M2 is reduced to about 0.48 m. M3 proposed in this paper has the highest positioning accuracy and the position error is about 0.07 m.

(ii) When $x,y\in[-100\text{ m},100\text{ m}]$, the underwater target position errors of M1, M2 and M3 within this area are about 0.53 m, 0.29 m and 0.05 m, respectively; when the underwater target is outside the deployment range of the LBL system, the underwater target position error increases rapidly, especially for M1 and M2. Therefore, M3 is

more stable. Besides, in the underwater target positioning test, it should be ensured that the underwater target is within the deployment range of the LBL system in order to obtain the high-accuracy underwater target position parameters.

According to the results above, it can be concluded that identifying the sound speed error can reduce the solution error in M1. However, M2 still regards the underwater sound speed as a constant, which is also an approximation of the underwater sound speed, so the improvement for the positioning accuracy is still limited. M3 approximates the underwater sound speed as a vertical layered model, and uses the constant gradient acoustic ray tracing to calculate the TOA of the acoustic signal between two underwater points. The new positioning solution has the highest accuracy, which coincides with the theoretical analysis.

6. Conclusions

Due to the variety of the underwater sound speed, the acoustic propagation path is a curve and the traditional LBL positioning algorithm brings the inevitable system error with constant sound speed, resulting in poor positioning accuracy. A TOA intersection positioning model based on the constant gradient acoustic ray tracing is built to reduce the change of the underwater sound speed on the positioning accuracy, and the feasibility of the model theoretically is analyzed. Moreover, the overall TOA residual square sum is constructed as the optimization function and the PSO algorithm is used to obtain the optimal estimation for the underwater target position parameters. Compared with the distance intersection positioning algorithm, the TOA intersection positioning algorithm can effectively improve the positioning accuracy of the LBL system from the simulations, which can provide a valuable reference for the underwater positioning test.

References

[1] LI H, LIU M Y, LIU K. Bio-inspired geomagnetic navigation method for autonomous underwater vehicle. Journal of Systems Engineering and Electronics, 2017, 28(6): 1203–1209.

[2] ZHAO D, SEONG W, LEE K, et al. Shallow water source localization using a mobile short horizontal array. Journal of Systems Engineering and Electronics, 2013, 24(5): 749–760.

[3] BALLU V, AMMANN J, POT O, et al. A seafloor experiment to monitor vertical deformation at the Lucky Strike volcano, Mid-Atlantic Ridge. Journal of Geodesy, 2009, 83(2): 147–159.

[4] URICK R J. Principles of underwater sound-2. New York: Mc Graw-Hill Book, 1975.

[5] SURVEYOR D M, GIOVANNI M. Underwater acoustic positioning system. Montana: Betascript Publishing, 2010.

[6] ARRICHIELLO F, HEIDARSSON H K, SUKHATME G S. Opportunistic localization of underwater robots using drifters and boats. Proc. of the International Conference on Robotics and Automation, 2012: 5307−5314.

[7] BINGHAM B, SEERING W. Hypothesis grids: improving long baseline navigation for autonomous underwater vehicles. IEEE Journal of Oceanic Engineering, 2006, 31(1): 209–218.

[8] ALCOCER A, OLIVEIRA P, PASCOAL A. Study and implementation of an EKF GIB-based underwater positioning system. Control Engineering Practice, 2007, 15(6): 689–701.

[9] ZHANG Y, LIANG J X, JIANG S M, et al. A localization method for underwater wireless sensor networks based on mobility prediction and particle swarm optimization algorithms. Sensors, 2016, 16(2): 212.

[10] CHAN Y T, HANG H Y C, CHING P. Exact and approximate maximum likelihood localization algorithms. IEEE Trans. on Vehicular Technology, 2006, 55(1): 10–16.

[11] YAN J, TIBERIUS C C J M, TEUNISSEN P J G, et al. A framework for low complexity least-squares localization with high accuracy. IEEE Trans. on Signal Processing, 2010, 58(9): 4836–4847.

[12] WANG Z M, YI D Y, DUAN X J, et al. Measurement data modeling and parameter estimation. Florida: CRC Press, 2016.

[13] ZHANG J C, HAN Y F, ZHENG C E, et al. Underwater target localization using long baseline positioning system. Applied Acoustics, 2016, 111: 129–134.

[14] XU P, ANDO M, TADOKORO K. Precise, three-dimensional seafloor geodetic deformation measurements using difference techniques. Earth, Planets and Space, 2005, 57(9): 795–808.

[15] MEDWIN H. Speed of sound in water: a simple equation for realistic parameters. The Journal of the Acoustical Society of America, 1975, 58(6): 1318–1319.

[16] JAMSHIDI S, ABU BAKAR M N B. An analysis on sound speed in seawater using CTD data. Journal of Applied Sciences, 2010, 10(2): 132–138.

[17] SUN D J, LI H P, ZHENG C E, et al. Sound velocity correction based on effective sound velocity for underwater acoustic positioning systems. Applied Acoustics, 2019, 151: 55–62.

[18] GENG X Y, ZIELINSKI A. Precise multibeam acoustic bathymetry. Marine Geodesy, 1999, 22(3): 157–167.

[19] XIN M Z, YANG F L, WANG F X, et al. A TOA/AOA underwater acoustic positioning system based on the equivalent sound speed. The Journal of Navigation, 2018, 71(6): 1431–1440.

[20] AMEER P M, JACOB L. Localization using ray tracing for underwater acoustic sensor networks. IEEE Communications Letters, 2010, 14(10): 930–932.

[21] LU X P, BIAN S F, HUANG M T, et al. An improved method for calculating average sound speed in constant gradient sound ray tracing technology. Geomatics and Information Science of Wuhan University, 2012, 37(5): 590–593.

[22] YAN W S, CHEN W, CUI R X. Moving long baseline positioning algorithm with uncertain sound speed. Journal of Mechanical Science and Technology, 2015, 29(9): 3995–4002.

[23] HUANG J, YAN S G. An improvement of long baseline system using particle swarm optimization to optimize effective sound speed. Marine Geodesy, 2018, 41(5): 439–456.

[24] KENNEDY J, EBERHART R. Particle swarm optimization. Proc. of the International Conference on Neural Networks, 1995, 4: 1942–1948.

[25] TANG M N, CHEN S J, ZHENG X H, et al. Sensors deployment optimization in multi-dimensional space based on improved particle swarm optimization algorithm. Journal of Systems Engineering and Electronics, 2018, 29(5): 969–982.

[26] LI H Z, WANG Y. Particle swarm optimization for rigid body reconstruction after micro-Doppler removal in radar analysis. Journal of Systems Engineering and Electronics, 2020, 31(3): 488–499.

[27] ZHANG X, WANG P, XING J C, et al. Particle swarm optimization algorithms with decreasing inertia weight based on Gaussian function. Application Research of Computers, 2012, 29(10): 3710–3712.

Biographies

XING Yao was born in 1997. He received his B.S. degree in applied mathematics from National University of Defense Technology, Changsha, China, in 2020. Currently, he is working toward his M.S. degree at the College of Liberal Arts and Sciences, National University of Defense Technology. His current research interests are data fusion, velocity measuring and positioning, systematic error identification, and target localization using underwater sound.
E-mail: y__1326@163.com

WANG Jiongqi was born in 1979. He received his B.S. degree in applied mathematics from Zhejiang University, Hangzhou, China, in 2002, and his M.S. and Ph.D. degrees in system science from National University of Defense Technology, in 2004 and 2008, respectively. He is a professor in the College of Liberal Arts and Sciences, National University of Defense Technology, Changsha, China. His research interests include measurement data analysis, parameter estimation, system identification, and space target state filter and its applications.
E-mail: wjq_gfkd@163.com

HE Zhangming was born in 1985. He obtained his B.S. and M.S. degrees in applied mathematics from National University of Defense Technology, Changsha, China, in 2008 and 2010, respectively. From 2013 to 2014, he was a visiting scholar in Institute for Automatic Control and Complex Systems, University of Duisburg-Essen, Duisburg, Germany. He obtained his Ph.D. degree in system science from National University of Defense Technology, in 2015. He is a lecturer since 2015 and an associate professor since 2019 in the College of Liberal Arts and Sciences, National University of Defense Technology, Changsha, China. His research interests include fault diagnosis and prognosis, signal processing, and system identification.
E-mail: hzmnudt@sina.com

ZHOU Xuanying was born in 1991. She received her B.S., M.S., and Ph.D. degrees in applied mathematics from National University of Defense Technology, Hunan, in 2013, 2016, and 2019, respectively. She is a lecturer at the College of Liberal Arts and Sciences, National University of Defense Technology, Changsha, China. Her research interests include system modelling, data processing, missiles, and signal process and its applications.
E-mail: Julia_chow07@163.com

CHEN Yuyun was born in 1979. She received her B.S., M.S., and Ph.D. degrees in applied mathematics from National University of Defense Technology, Changsha, Hunan, in 2002, 2004 and 2017, respectively. She is a professor in the School of Mathematics and Big Data, Foshan University. Her main research interests include data analysis, nonlinear filter, and parameter estimation.
E-mail: kasineya@sina.com

PAN Xiaogang was born in 1979. He received his Ph.D. degree in applied mathematics from National University of Defense Technology in 2009. He is a professor and master's supervisor. His main research interests are mission planning and operational research analysis.
E-mail: panxiaogang_nudt@163.com